PCCP

Accepted Manuscript

ROYAL SOCIETY OF CHEMISTRY

rsc.li/pccp

View Article Online
DOI: 10.1039/C7CP08498F

Journal Name

ARTICLE TYPE

Cite this: DOI: 10.1039/xxxxxxxxxx

Nitrogen Doped Nanohoops as Promising CO_2 Capturing Devices

Angel Vidal Vidal,[a] Carlos Silva López,[a] and Olalla Nieto Faza*[b]

Received Date
Accepted Date

DOI: 10.1039/xxxxxxxxxx

www.rsc.org/journalname

The impact of climate change in the face of steady or increasing emissions has made the capture and storage of CO_2 a priority issue. Supramolecular chemistry is one of the tools that can be used for this task, due to the possibility of tuning intermolecular interactions for the capture of this gas in a selective and efficient way. In this context, this work presents a novel approach for the capture of CO_2 based on n-cycloparaphenylenes ([n]-CPPs) doped with nitrogen atoms. This is the first time that the potential of these structures for the capture of polluting gases has been evaluated. Among all the structures analysed, the one yielding the best results (complexation energy of -32,80 kJ/mol) contains 4 nitrogen atoms per monomer. The topology of the electron density of the host-guest complex and the nature of its non-covalent interactions have been analyzed in this work in order to explain this high binding energy and identify potential structural modifications to improve it. The capability of this system to be used as a sensing device for CO_2 using vibrational spectroscopy is also explored.

1 Introduction

Nanohoops, chemically known as [n]cycloparaphenylenes ([n]-CPPs) are closed macrocyclic molecules formed by *n* benzene units linked at the para position, resulting in a rigid three-dimensional architecture that in solid state forms long-range channels [1–4] with multiple π-π contacts. [5,6] Cycloparaphenylenes were termed *carbon nanohoops* in 2008 by Jasti and Bertozzi and represent the smallest structural unit of armchair carbon nanotubes (CNTs). [7–10] They can also be regarded as the link between small oligomers and phenylene polymers. [n]CPPs possess a unique, rigid, full sp^2-hybridized conjugated core with a radially oriented π system [11] which provides a hydrophobic electron-rich cavity that acts as a strong host for electron-deficient guests. [12–15] The closed ring structure of [n]-CPPs provides them with several advantageous properties in relation to their linear counterparts, such as diameter-dependent optoelectronic properties [16–19], a narrowing of the HOMO-LUMO gap, [11] size-dependent fluorescence, [5,19,20] and molecular recognition capabilities or the ability to capture and storage different molecules. [15]

Nanohoops were first envisioned in 1933 by Parekh and Guha, many years prior to the discovery of CNTs. [21] Although they possess a simple structure, the synthesis of [n]-CPP has represented a significant challenge to experimentalists due to their high strain energy, and almost 75 years were needed for this task to be accomplished. [22] In 2008 Bertozzi and Jasti [8] reported the first synthesis of [n]-CPP, which was shortly followed by that of the Itami group, [23] who published the first size-selective synthesis some months later. Yamago et al. [24] also proposed an alternative procedure in 2010. The synthetic methodology to address the high structural strain problem is based on the initial formation of unstrained macrocyclic precursors followed by either a reductive aromatization (Bertozzi and Jasti [8]), an oxidative aromatization (Itami [23]) or a reductive elimination (Yamago [24]) to achieve the formation of [n]-CPPs. Since the first synthetic procedure was described 9 years ago, [5]-[16]-CPP and also [18]-CPP with several substituted analogues have been reported. [4,23,25–28] After the first [n]-CPP was synthetically produced, numerous experimental studies based on size-dependent properties have been elucidated, nonetheless, not much attention has yet been paid to the study of this structure as host for other molecules.

There have been some attempts of doing host-guest chemistry in similar systems such as cycloparaphenyleneacetylenes (CPPAs) but they were mainly focused on the study of convex–concave π-π interactions. [29]. For example, Kawase *et al.* have described the complexation of CPPAs with fullerenes in several studies, [30–32] and some guest-host complexes between a differ-

[a] *Departamento de Química Orgánica. Universidade de Vigo. Lagoas-Marcosende s/n. 36211, Vigo, Spain*
[b] *Departamento de Química Orgánica. Universidade de Vigo. Campus As Lagoas, 32004, Ourense, Spain. Tel 34 9883 6888; E-mail: faza@uvigo.es*

† Electronic Supplementary Information (ESI) available: Structures of the studied CO_2-nanohoop complexes are shown. See DOI: 10.1039/b000000x/

View Article Online
DOI: 10.1039/C7CP08498F

ent number of CPPAs and fullerenes in onion or matryoshka-type systems have also been reported.[30] In the case of [n]-CPPs there are some published investigations concerning the complexation of fullerenes[14,33] and metallofullerenes such as (La@C82)@[11]-CPP[12] and (Li^+@C60)@[10]-CPP.[13] A very recent work by Della Sala and coworkers studies the application of the [8]-CPP macrocycle towards the recognition of pyridinium cations,[34] but smaller rings have never been used as hosts for small molecules.

In this study, we analyze the affinity of these structures for the carbon dioxide molecule with the aim of developing novel capture and/or sequestration systems. CO_2 is a greenhouse gas[35,36] at the root of several environmental issues such as global warming and climate change.[37–39] For the past 1 million years the atmospheric concentration of CO_2 has been kept more or less constant around 200 ppm but already in 2017 the amount of CO_2 in the atmosphere has exceeded 400 ppm. Thus, finding ways to decrease the concentration of this pollutant in the atmosphere is one of the most important issues that humanity has to tackle in the XXI century.[40] Traditional ways of removing CO_2 from raw industrial feedstocks are outdated, so the search for new and more sophisticated strategies such as high selective materials with specific and tunable properties are highly desired.

The high affinity of CO_2 for nitrogen atoms is well known and it is the basis of the traditional methods for the capture of this gas: absorption using nitrogen-based solutions.[41–43] Moreover, it has also been demonstrated that substituted heteroaromatic systems have enhanced CO_2 binding energies in supramolecular complexes.[44,45] Based on this knowledge, we propose in this work the use of nitrogen doped nanohoops (aza-[6]-CPPs) as novel structures for CO_2 capture (Figure 1). We expect that the adition of nitrogen atoms will enhance binding energies with respect to the all carbon [6]-CPP. The [6]-CPP nanoring was chosen as the parent system for our structural modifications because of the size of CO_2 and the distances that it will have to its interaction partners once inside the cage. As the stabilization of carbon dioxide inside the cage is mediated by non-covalent interactions, the size of the ring is expected to play a major role.

To achieve this objective and evaluate the ability of these structures for the capture and storage of CO_2, *ab-initio* computational chemistry methods are used.

2 Computational Methods

Density Functional Theory in the Kohn-Sham formulation as implemented in Gaussian 09[46] has been employed to locate minima on the potential energy surfaces of the complexes under study. All calculations have been done with the dispersion corrected hybrid-meta GGA functional M06-2X[47] in combination with the Ahlrich's triple-ξ quality basis set including polarization functions def2-TZVPP.[48,49] To achieve high accuracy results, tight self-consistent field criteria and an ultrafine pruned grid (99,590) for the numerical integration have been used. The latter consists of 99 radial shells and 590 angular points per shell. All calculations have been done in gas phase and the stability of the wavefunction has been computed for all stationary points found.[50,51] Harmonic analysis of the second derivatives of the energy with respect to the nuclear

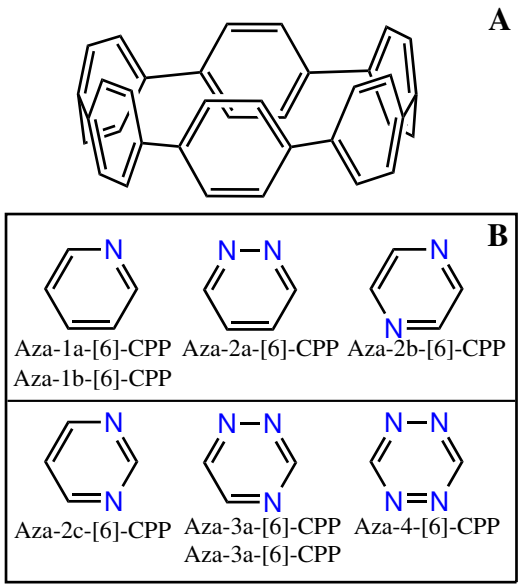

Fig. 1 A: Chemical structure of the full-carbon [6]-cycloparaphenylene used as the parent system in this study. B: Different heterocyclic monomers used in the proposed structural modifications. Note that both the pyridine and the 1,2,4-triazine ring have two nomenclatures: Aza-1a-[6]-CPP and Aza-1b-[6]-CPP for the first and Aza-3a-[6]-CPP and Aza-3b-[6]-CPP for the second. Although the base heterocycle is the same, there are different ways of linking them together. In the case of the pyridine ring (arrangement 1b) it is actually a 3-membered homopolymer formed by three 2,2'-bipyridine molecules, whereas the system 3b is a homopolymer obtained through the bonding of three units of 6,6'-bi (1,2,4-triazine).

displacements has also been performed to ensure that a minimum structure and not a transition state has been found. Binding energies have been computed within the supermolecule approach and subsequently corrected with the counterpoise procedure described by Boys and Bernardi.[52] Topological analysis based on the Quantum Theory of Atoms in Molecules (QTAIM)[53–56] has been performed with the open source software Multiwfn[57] with the wavefunctions previously obtained using Gaussian 09.[46]

3 Results and discussion

For the construction of the initial structure of the nanohoop we have used the crystallographic data deposited by Jianlong et al in CCDC (CCDC-852989).[2,58] A single ring has been extracted from the crystal structure and optimized at increasingly higher levels of theory until reaching M06-2X/def2-TZVPP. This optimized structure has been used as a template in the construction of the other nanohoops in this work, through the doping of the structure with nitrogen atoms. The spatial arrangement chosen for these nitrogen atoms, however, is not fortuitous and the *para* positions, at which the heterocycles are bonded, have been left unaltered in all structures at this stage of the project, in order to avoid charges and counter ions in the systems.

The doped structures thus built have been reoptimized at the same level of theory. Once they have been optimized, a CO_2 molecule has been placed inside each of them in a random position and the resultant complex has been re-optimized until a

View Article Online
DOI: 10.1039/C7CP08498F

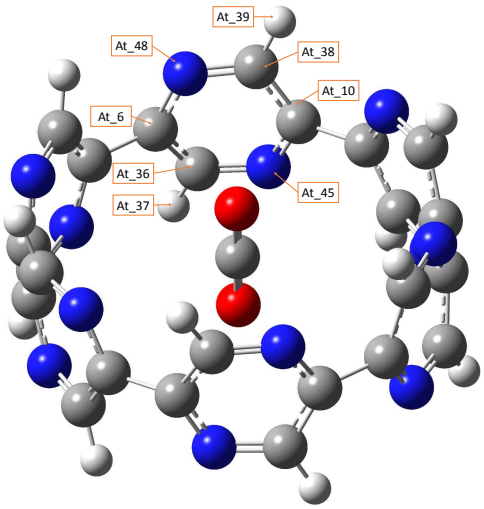

Fig. 2 Different orientations considered in the sampling of the aza-2a-[6]-CPP doped with two nitrogen atoms. Due to the symmetry of the system only 8 different directions need to be considered. Atom labels (At-48, At-39 and so on) correspond to the orientation of the CO_2 rotation according to the Euler-Rodrigues formula.

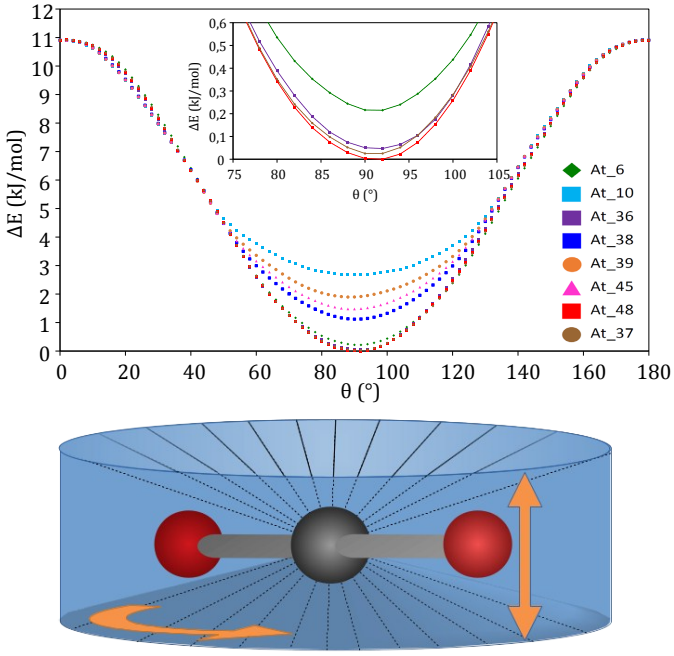

Fig. 3 Energy vs. CO_2 rotation angle for the CO_2-aza-2a-[6]-CPP complex at different orientations. These values are expressed in kJ/mol as relative energies with respect to the global minimum. The inset highlights the region between 75° and 115 °, which surrounds the global minimum. The global minimum can be found in this insert for the orientation At-48. Three other orientations are close in energy to At-48 and display minima close to the global minimum: At-37 (+ 0.03 kJ/mol), At-36 (+0.05 kJ/mol) and At-6 (+0.22 kJ/mol). Relative energies for the minima found at the other orientations are: +1.12 kJ/mol in At-38, +1.49 kJ/mol in At-45, +1.91 kJ/mol in At-39 and +2.68 kJ/mol in At-10. The lower panel shows a schematic representation of the free tumbling expected at room temperature for the CO_2 molecule inside the nanohoop, inferred from the calculated energy profiles.

minimum in the potential energy surface has been reached. This procedure has been repeated 5 times for each structure obtaining in all cases the same position of the carbon atom, but slight variations in the orientation of the oxygen atoms of CO_2. One of the problems when dealing with this type of supramolecular structures is based on the existence of multiple relative minimums on the potential energy surface (PES), so to make sure that we are facing a global minimum on the PES and not a relative one, systematized sampling of this surface has been done. For doing this sampling, we have placed in each complex the CO_2 carbon in its optimal position and subsequently, oxygen atoms have been arranged parallel to the heterocycles that form the aza-[6]CPP structure. From this position the CO_2 molecule has been rotated inside the cell at intervals of 2 degrees, following different directions on the three dimensional space using the Euler-Rodrigues formula.[59] The implementation of this algorithm is a well-known and efficient procedure for rotating a vector in space (the CO_2 molecule in this case), given an axis and angle of rotation. The rotation axis is used as the direction to which the CO_2 molecule is moving and is defined using different atoms on nanohoop structure as labelled in Figure 2.

The results of this sampling of the potential energy surface of the complexes are shown for Aza-2a-[6]-CPP, doped with two nitrogen atoms, in Figures 2 (where we showcase the different orientations that have been considered for CO_2 inside the macrocycle) and 3 (where relative energies with respect to the global minimum are plotted at different angle values for each orientation).* The minimum for this supramolecular complex its found at a rotation of 92° with respect to the initial configuration in the At-48 orientation. Among the 8 sampling directions considered, 3 groups can be made considering the relative energies or their minima. The first one includes those orientations for which the energies with respect to the global minimum (the reference) are less than 0,30 kJ/mol (4 orientations); the second, those whose relative energy is between 1 and 2 kJ/mol higher than the reference (3 orientations); and the third, those whose relative energies exceed 2 kJ/mol (1 orientation).

When looking at the results of these energy profiles, we find that the relative energies of the minima are very close to each other, and even the most unfavourable configuration does not exceed 25 kJ/mol in any aza-doped system, which shows that the potential energy surface is fairly smooth for CO_2 inside these structures. As a result, at room temperature, the captured CO_2 molecule can easily tumble inside the nanohoop visiting without significant penalty θ values from about -45° to 45° in all the orientations considered. Thus, inside this revolution volume CO_2 would be able to pivot and rotate almost freely (see Figure 3) exhibiting a molecular gyroscope behavior as reported in other similar systems in the literature[60–62].

It is worth noticing, however, that the energy difference between the more and less favourable configurations increases with

* The equivalent plots for the other macrocycles in this study labelled according to the orientations followed in the potential energy surface sampling can be found in the Supporting Information.

View Article Online
DOI: 10.1039/C7CP08498F

Table 1 Binding energies (BE) corrected for the basis set superposition error as obtained with the supermolecule approach. This procedure is based on subtracting the energy of the empty ring and also the energy of the CO_2 molecule from the energy of the complex. The second column contains the Gibbs free energies for the CO_2 capture calculated at room temperature. The *orientation* colum provides the rotation angle (in degrees) of CO_2 at which the global minimum of the potential energy surface is found, while *direction* indicates the atom that determines the rotation axis. The table also shows the number of total nitrogen atoms in the ring (the number of nitrogen atoms per monomer can be obtained by dividing the total number by 6 or from the system name itself). The second to last and penultimate columns display, respectively, the BSSE corrected BE of nitrogen inside the nanohoop, and the complexation free energy at room temperature. The last column shows the strain energy for the doped nanohoop rings obtained through a homodesmotic reaction (see text for details). Note that all energies included in this table are expressed in kJ/mol. [a]

System	BE_{CO_2}	ΔG_{CO_2} (298K)	Orientation	Direction	# N atoms	BE_{N_2}	ΔG_{N_2} (298K)	Strain energy
[6]-CPP	-18.83	12.94	71°	Atom 9	0 N	-16.90	15.30	365.82
Aza-1a-[6]-CPP	-22.01	11.97	88°	Atom 53	6 N	-17.67	7.42	317.50
Aza-1b-[6]-CPP	-28.03	9.27	48°	Atom 44	6N	-16.07	8.28	341.56
Aza-2a-[6]-CPP	-25.69	12.22	92°	Atom 48	12 N	-19.33	13.13	294.20
Aza-2b-[6]-CPP	-25.86	8.41	114°	Atom 47	12 N	-19.54	12.13	336.31
Aza-2c-[6]-CPP	-24.10	12.46	90°	Atom 42	12 N	-17.95	13.41	300.98
Aza-3a-[6]-CPP	-29.58	7.96	86°	Atom 16	18 N	-20.84	10.99	258.23
Aza-3b-[6]-CPP	-29.54	6.67	94°	Atom 7	18 N	-20.88	10.82	356.11
Aza-4a-[6]-CPP	-32.80	-2.19	88°	Atom 39	24 N	-22.59	5.31	238.32

[a] The binding free energies for the complexation process have to be taken with a grain of salt because of the undue effect of the low frequency vibration modes treated within the harmonic approximation.

the number of nitrogen atoms in the system. These results indicate the paramount importance of the number and position of nitrogen atoms in the structure in modifying the strength of the interactions that are established between the host and the guest.

Using the global minimum configurations obtained through the systematic sampling of the potential energy surface just described, we have carried out full optimizations to locate the actual global minima. With these structures, we have calculated the binding energy between CO_2 and the different nanohoops. The values of these binding energies are summarized in Table 1. Binding energies display the same trend we found when evaluating the differences between the most and less favourable configuration in the previous sampling: as the degree of doping with nitrogen increases, binding energies are higher.

Because the BSSE binding energies reported in Column 1 of Table 1 do not take into account the effect of thermal energy on binding we have also computed BEs in terms of Gibbs Free Energies. This way, we can give a more realistic view of the complexation process and analyse the effects of the temperature on it. At room temperature the binding energies of the nanohoops considered vary between +12.94 kJ/mol in [6]-CPP and -2.19 kJ/mol in aza-4-[6]-CPP, being this last one the only system which possesses a negative complexation energy at 298K. The entropic component of the Gibbs free energy causes complexation energies to decrease as the temperature raises. Nonetheless these data do not imply that the systems cannot be used in technological applications, since both temperature and pressure in effluents are controllable parameters that can be set to favour the binding process.

Which of the different structural isomers is chosen also affects the binding energies, but this effect is not as dramatic as in the case of the number of heteroatoms added to the structure. Based in these results, the most promising structure is the nanohoop doped with four nitrogen atoms (aza-4-[6]-CPP).

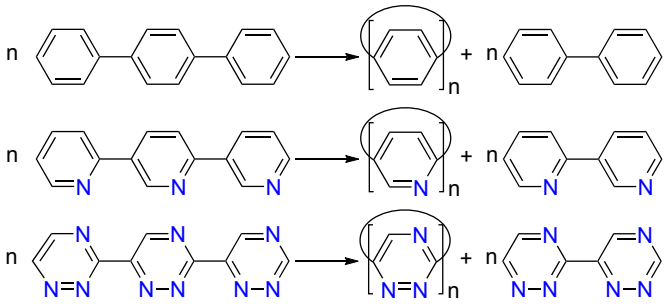

Fig. 4 Examples of the homodesmotic reactions used for the calculation of the strain energy of aza-doped nanohoops. These reactions are similar to those reported by other authors in the literature[63,64] and have been suitably modified to take into account the substitution pattern with nitrogen atoms on each particular ring.

Since nanohoops doped with a large number of nitrogen atoms have not been synthesized yet, it is interesting to analyse the plausibility of their preparation. For macrocyclic systems strain energy is usually directly related to their stability and viability, so we used the strain energies of our nitrogen-doped nanohoops, and their comparison with those of [n]-CPPs, which have already been synthetized, to analyze the viability of a hypotetical synthetic process. Strain energies were calculated using a homodesmotic reaction analogous to that reported by Bachrach *et al.*[63] and Segawa *et al.*[64] modified to take into account the number of nitrogen atoms in the structure and their spatial arrangement, as shown in Figure 4. Note that an equivalent reaction group that preserves the number of substituted rings in para positions and also the Benson group equivalents are used to this purpose. The results obtained (displayed in the last column of Table 1) are computed using thermal corrected Gibbs Free energies at 298K. The different positional isomers have different strain energies, a result that is consistent with those reported by Bachrach *et al.* Taking the average value of the strain energies for systems with the same amount of nitrogen it can be seen that the mean value of the strain energy decreases (from 365.82 kJ/mol in the [6]-CPP system to 238.32 kJ/mol in the structure with the largest bind-

View Article Online
DOI: 10.1039/C7CP08498F

ing energy: aza-4-[6]-CPP) as the degree of doping increases. The intermediate values for systems with 1N, 2N and 3 nitrogen atoms are respectively 329.53 kJ/mol, 310.50 kJ/mol and 307.17 kJ/mol. Considering these values, strain shouldn't preclude the preparation of the doped structures, particularly of the one with the most promising BE, aza-4-[6]-CPP.

In the absorption processes of polluting gases, one of the main drawbacks is the existence of competitive guests that saturate the binding sites, resulting in the effectiveness of the absorbent structure being usually lost. In the case of CO_2, nitrogen is usually a competitive molecule, not only because of its chemical characteristics but also because of its abundance in the atmosphere. To study selectivity, the same procedure and level of theory described for CO_2 was used with N_2 (Table 1). The CO_2/N_2 ratio in terms of binding energies provides information about the selectivity of these structures with respect to CO_2 capture. When looking at these values, a trend is found, with selectivity for CO_2 decreasing upon increasing the number of nitrogens on the nanohoop structure. The ratios are quite high across the entire series and range from 0.90 for [6]-CPP to 0.69 for Aza-[6]-4-CPP. The selectivity however is quite sensitive to particular arrangements of the nitrogen atoms (0.80 for aza-1a-[6]-CPP vs. 0.57 for aza-1b-[6]-CPP). With these results at hand we can expect considerable selectivity at low temperatures. We have also evaluated the complexation energies at 298K and the results can be found in Table 1. Interestingly no nitrogen complex is stable when thermal energies are considered, which suggests that selectivity could be enhanced at room temperature due to nitrogen becoming non-competitive.

There are some investigations describing the properties and uses of nanohoops doped with nitrogen atoms.[7,11,65,66] Bachrach and Stück have also studied computationally the conformations and strain energies for rings with 1 and 2 nitrogen atoms and sizes ranging from 3 to 24 heterocyclic monomers.[63] However, as far as we know, neither rings with more than two nitrogen atoms per monomer, nor the effects of these heteroatom substitutions on binding energies have been studied either computationally or experimentally. Since the structure aza-[6]-CPP composed by 1,2,4,5-tetrazine monomers displays the best CO_2 binding energy, the characterization of the structure of the complex and a deep analysis of the intermolecular interactions which stabilize it, has been performed on this system.

QTAIM is based on the analysis of the topological features of the molecular electron density distribution ρ,[53–56] which permits a definition of the principal objects in molecular structures, such as atoms and bonds, using the properties of this observable (ρ). Nuclear, bond and ring critical points (CPs) are mathematical singular points of ρ. By analyzing the potential energy density $V(r)$, the Lagrangian of the kinetic energy $G(r)$, and also the Laplacian of the electron density at the bond critical point, a classification of the bonds based on their nature[67–69] can be established. Table 2 shows the average value of the mentioned properties at the four CPs found between CO_2 and the nanohoop. The average value of the Laplacian ($\nabla^2\rho(BCP)$) is higher than zero, as is the sum of G(BCP) + V(r) (that is, the energy density), which implies the existence of a weak interaction. A graphical representation of the QTAIM and topological analysis can be seen on Figure 5.

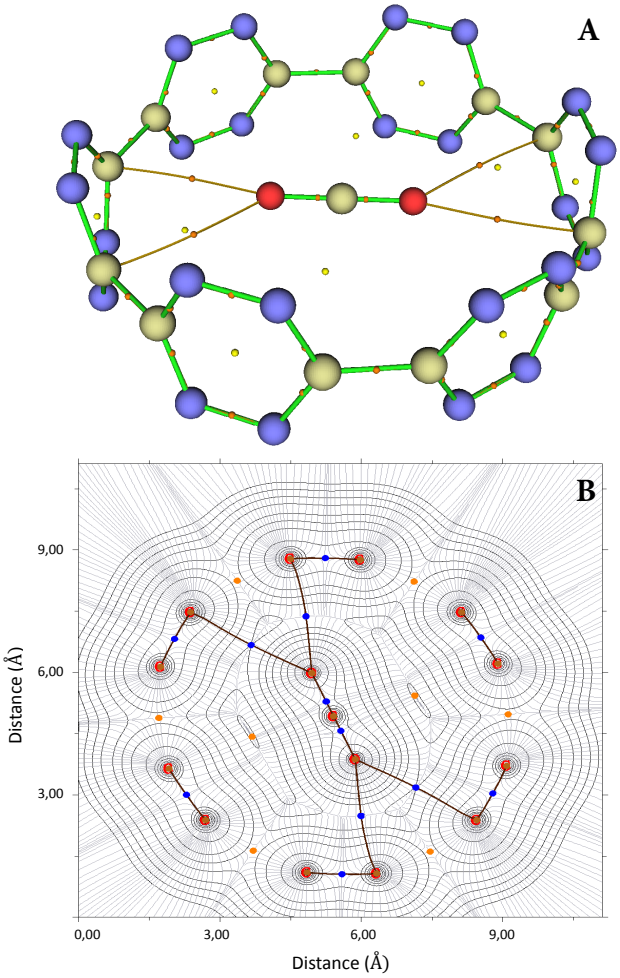

Fig. 5 Figure A shows the QTAIM critical points (CPs) for the Aza-4a-[6]-CPP structure: ring CPs in yellow, and bond CPs in orange. It also displays (orange) the paths connecting the oxygen atoms (nuclear CPs) with the nuclear CPs of some carbon atoms of the host, passing through four bond critical points (information about these four CPs can be found in the text). Figure B represents the results of the topological analysis of the electronic density of aza-4a-[6]-CPP on the plane that includes the main axis of the CO_2 molecule. Tick labels are associated to distances in Å, while contours (black lines) correspond to electron density values of 0.002, 0.004, 0.008, 0.020, 0.040, 0.080, and so on, starting from the outside. Gradient lines (grey) are also shown, to visualize the attraction basins.

Table 2 Averaged properties at the four critical points that lie between CO_2 and the host. Values are displayed in atomic units (a.u.).

Property	Symbol	Average value (a.u.) x10^{-3}
Lagrangian Kinetic energy	G(r)	8.126
Hamiltonian Kinetic energy	K(r)	-1.765
Potential energy density	V(r)	-6.361
Energy density	H(r)	1.765
Laplacian of electron density	$\nabla^2\rho$	3.956

View Article Online
DOI: 10.1039/C7CP08498F

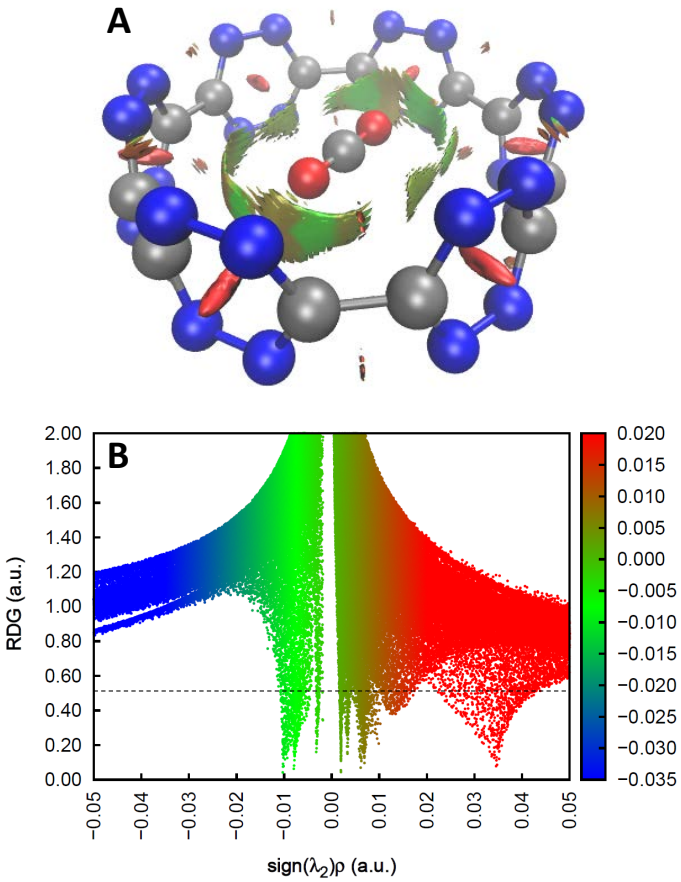

Fig. 6 Figure A: representation of the non-covalent interactions analysis for the structure aza-4a-[6]-CPP. This colour chart serves to distinguish first, the region in which non-covalent interactions appear and second, to discriminate type of interaction. This representation shows the 0.5 isosurface of the Reduced Density Gradient (RDG) and is coloured on a blue-green-red scale according to values of sign (λ_2)rho, ranging from -0.04 to 0.02 au. Green corresponds to weak van der Waals interactions (vdW), blue indicates strong, attractive interactions (such as hydrogen bonds, if present) and red implies non-bonded overlap like steric effects. Figure B shows the scatter graph between the RDG and the electron density multiplied by the second largest eigenvalue of the Hessian matrix of electron density (called λ_2). This graphical representation also showcases the non-covalent interactions in this system and confirms both the existence of a large presence of vdW interactions(in its central region) and the existence of steric interactions (in the region of positive values in the X axis). The black dotted line shown on this figure represents the isosurface value chosen for the graphical representation in Figure 6 A. The most common isosurface used for NCI representations is 0.5, but moving up and down this line other isosurfaces can be represented. To facilitate the interpretation, the color code used for this representation is the same as that of subfigure A.

In order to have a better knowledge of the type of interaction, a non-covalent interaction analysis was performed. Non-covalent interactions (NCI) have a unique signature and their presence can be revealed solely from the analysis of the electron density.[70] It must be kept in mind that NCI are highly nonlocal and manifest in real space as low-gradient isosurfaces with low density, so NCI can be located by generating gradient isosurfaces enclosing the corresponding regions of real space. To discriminate the type of interactions, low-density and low-gradient regions cannot be used alone.[70] The sign of λ_2 eigenvalue (see Figure 6) can be used to distinguish bonded from nonbonded interactions and the electron density itself provides information about their strength, so the product of the sign of λ_2 by the electron density provides a lot of information about both the strength and the type of interaction.[71,72] In Figure 6 the 0.5 a.u. isosurface is represented and a colour scale is adopted, ranging from blue (in the case of strong bonding interactions such as hydrogen or halogen bonds) to red (in the case of strong repulsions due to steric effects) passing through green for weak van der Waals interactions. This analysis reflects that there are only weak, non-covalent van der Waals interactions between CO_2 and the ring structure and also reveals the presence of steric repulsive interactions between the tetrazine rings. The scatter graph between the RDG and the sign $(\lambda_2)\rho$ (Figure 6 B) allows us to confirm the type of interactions and their intensity as a function of the chosen isosurface.

The reason why the capture of carbon dioxide is effective in nitrogen-doped nanohoops is based on the existence of multiple weak additive interactions that as a whole greatly stabilize the guest inside the cavity.[73,74] In this type of supramolecular systems the complexation of the guest is usually achieved through interaction with the global electronic density of the ring, so, the effect of a larger number of nitrogen atoms in the nanohoop seems to be a richer electronic density that interacts in a stronger way with the guest.

Despite the fact that CO_2 capture by nitrogen-containing systems is usually mediated by Lewis-layer-base interactions, in this case they are not present. When this type of interaction occurs the CO_2 carbon (that is electron-deficient) interacts with an electron-donor functional group with which it establishes a very favourable donor-acceptor interaction, usually changing the angle of the CO2 molecule. As an example, the CO2 angle in the aza-4-[6]-CPP system is 179.998°, which suggests no Lewis acid/base interactions occurring in the complex. Although such an interaction would be individually more favourable than any of those actually found in the complex, the wekaer interactions found between CO_2 and the aromatic rings in the optimal structure are additive, and their number is maximized in this configuration.

To study the complexation of CO_2 (whether the structure is full or empty, the number of CO_2 molecules inside etc.) different spectroscopic techniques can be used. NMR spectroscopy, due to its sensitivity, could be the method of choice, but it is not a feasible alternative, out in the field, due to the instrumental needs and operation costs, since the ultimate goal of these capture systems is the sequestration of CO_2 in a wide set of environments (such as industrial effluents). An interesting property of nanohoops that could be exploited analytically is their intrinsic fluorescence, however, this property is only manifested in rings of sizes equal to or greater than 7 monomers ([7]-CPP).[5,19,20] As a result, despite its simple requirements, in situ application of this technique is not possible in this case. Thanks to the rigid full sp^2 conjugated core of nanohoops, UV-Vis spectroscopy is a very attractive technique to use for identification purposes. But, since CO_2 is not a chromophore, the differences in the signals between the complexed system and the empty structure are not significant and this sensitivity problem makes it difficult to work with this technique.

View Article Online
DOI: 10.1039/C7CP08498F

These considerations point towards vibrational spectroscopies as a good tool for the monitoring of complexation in these systems. Despite having a very simple structure, CO_2 features five very characteristic signals in its vibrational spectrum (see Table 3).

Table 3 Summary of vibrational modes for CO_2 in both gas phase and complexed within the nanohoop. All values are expressed in cm^{-1}. Note that the vibration ν_2 is decomposed in two (ν_{2a} and ν_{2b}) as a function of the plane in which the bending occurs. This vibration is degenerated in the gas phase but not in the complex. This spectroscopical signature can be used to analyze the degree of interaction between the guest and the host. See the text for more information.

ν_3	Type of vibration	Active	CO_2 gas	CO_2 at Aza-4a-[6]-CPP
ν_{c-}	Fermi resonance	Raman	1350,38	1344,04
ν_{c+}	Fermi resonance	Raman	1454,92	1454,94
ν_{2a}	Bending	IR	696,14	682,20
ν_{2b}	Bending	IR	696,14	696,09
ν_3	Asymmetric	IR	2448,09	2449,10

The asymmetric stretching vibration (present at 2449.10 cm^{-1} in aza-[6]-nanohoop) is an active very intense signal in IR spectroscopy. It should be noted that this structure only has C-C, C-N and N-N bonds whose characteristic vibrations are below 1550 cm^{-1}, so, in order to be able to differentiate if the cells are empty or filled with CO_2, it is enough to analyse if in the region between 2440 cm^{-1} and 2460 cm^{-1} there is an intense signal or not. On the other hand, the degenerated in gas phase bending vibration (696.14 cm^{-1} according to our calculations), is also active in IR but remarkably less intense. When CO_2 is complexed within the nanoring, this vibration is splitted into two different ones (ν_{2a} and ν_{2b}) and the separation between them depends on the degree of interaction of CO_2 with the nanohoop. The CO_2 molecule also has another characteristic spectroscopical signature called Fermi resonance.[75,76] This phenomenon appears due to the coupling of a fundamental vibration band (ν_1 at 1420,69 cm^{-1} in the nanohoop) with an overtone that is close in energy ($2\nu_2$=2x689,15 cm^{-1}). This causes that, in Raman spectroscopy, instead of a single intense signal a doublet appears (bands ν_{c-} and ν_{c+}). Those bands in the CO_2@aza-4a-[6]-CPP are located at 1344.04 cm^{-1} and 1454.00 cm^{-1} respectively, whereas in the case of free CO_2 these bands are located at 1350.38 cm^{-1} and 1454.92 cm^{-1}. Because a harmonic model is used in the calculation of the vibrational spectra, it is not possible to obtain the values for the Fermi resonance directly. For this it would be necessary to employ anharmonic corrections that are not feasible for systems of this size. For that reason, a perturbative treatment has been used for the calculation, which is a standard analytical procedure with negligible computational cost and rather accurate results as it has been demonstrated in the literature.[77,78]

To check the thermal variation of all the relevant IR signals in the complex, we simulated the effect of the conformational flexibility of CO_2 inside the nanohoop. Structures every 10 degrees of the rotation profile of CO_2 (in addition to the global minimum reported) were taken and we followed the procedure described in the Computational Methods section to compute the corresponding signals for all the bands reported on the manuscript. Assuming an equal participation of all the species considered (a worst case scenario implying that all conformations are isoenergetic) the average value and the standard deviation for each band were computed. The ν_{c-} band in the minimum energy configuration is hardly modified by the conformational freedom of the CO_2 inside the cell, since the average for all the spatial dispositions considered is at the same wave number value and the STD is lower than the resolution of some commercial spectrometers (2 cm^{-1}). The strategy of identification is also based on the fact that the Fermi resonance bands are narrow and very intense, so taking into account the thermal heterogeneous broadening of the bands, their high intensity would allow the analysis even in less than perfect thermal scenarios. Something similar happens with the ν_3 band: its average value is quite close to the value of the band at the minimum energy configuration, and the absence of other bands in the spectroscopic window would allow its easy identification. A band that suffers major changes is ν_{2a}, its average value 5.6 cm^{-1} larger than that calculated for the minimum energy configuration (692.8 cm^{-1}). Despite this, since this band appears at 696.14 cm^{-1} in the gas phase, there should be enough separation to allow identification (See the "Thermal broadening" section in the Supporting Information for the values).

4 Conclusions

In this work we use DFT calculations to demonstrate for the first time the potential of [6]-CPPs to act as host for CO_2 capture. After a sampling of the potential energy surfaces of CO_2 complexed with different nanohoops to find the global minimum energy configurations we find that doping the structure with nitrogen atoms greatly improves the binding energies of CO_2, which increase with the number of nitrogen atoms. On the global minimum structure of the best candidate, a detailed study has been carried out of the topological features, non-covalent interactions and spectroscopic properties. In order to characterize the nature of the host-guest interactions in this structure (mainly van der Waals-type interactions) and their relevance, QTAIM theory and NCI interaction analysis based on the reduced gradient density have been used. Such a detailed analysis is useful for tuning the intermolecular guest-host interactions so that we can create systems with enhanced binding energies. This type of work is currently being carried out in our research group. Finally, we propose the use of vibrational spectroscopy (both IR and Raman) to monitor the complexation process, and the potential of this supramolecular complex as a sensing device for CO_2.

5 Acknowledgements

The authors thank the Centro de Supercomputación de Galicia (CESGA) for the generous allocation of computer time, and the Ministerio de Economía y Competitividad (MINECO, PCTQ2016-75023-C2-2-P) and the Xunta de Galicia (ED431C2017/70) for funding. A. Vidal-Vidal is grateful to the Universidade de Vigo for a predoctoral fellowship.

Conflict of interest

There are no conflicts of interest to declare.

View Article Online
DOI: 10.1039/C7CP08498F

References

1 Y. Segawa, S. Miyamoto, H. Omachi, S. Matsuura, P. Senel, T. Sasamori, N. Tokitoh and K. Itami, *Angew. Chem. Int. Ed.*, 2011, **50**, 3244–3248.
2 J. Xia and R. Jasti, *Angew. Chem. Int. Ed.*, 2012, **51**, 2474–2476.
3 S. Yasutomo, S. Petr, M. Sanae, O. Haruka and I. Kenichiro, *Chem. Lett.*, 2011, **40**, 423–425.
4 E. Kayahara, Y. Sakamoto, T. Suzuki and S. Yamago, *Org. Lett.*, 2012, **14**, 3284–3287.
5 E. R. Darzi and R. Jasti, *Chem. Soc. Rev.*, 2015, **44**, 6401–6410.
6 M. R. Golder and R. Jasti, *Acc. Chem. Res.*, 2015, **48**, 557–566.
7 E. R. Darzi, E. S. Hirst, C. D. Weber, L. N. Zakharov, M. C. Lonergan and R. Jasti, *ACS Cent. Sci.*, 2015, **1**, 335–342.
8 R. Jasti, J. Bhattacharjee, J. B. Neaton and C. R. Bertozzi, *J. Am. Chem. Soc.*, 2008, **130**, 17646–17647.
9 H.-B. Li, A. J. Page, S. Irle and K. Morokuma, *J. Am. Chem. Soc.*, 2012, **134**, 15887–15896.
10 H. Omachi, T. Nakayama, E. Takahashi, Y. Segawa and K. Itami, *Nat. Chem.*, 2013, **5**, 572–576.
11 J. M. Van Raden, S. Louie, L. N. Zakharov and R. Jasti, *J. Am. Chem. Soc.*, 2017, **139**, 2936–2939.
12 T. Iwamoto, Z. Slanina, N. Mizorogi, J. Guo, T. Akasaka, S. Nagase, H. Takaya, N. Yasuda, T. Kato and S. Yamago, *Chem. Eur. J.*, 2014, **20**, 14403–14409.
13 H. Ueno, T. Nishihara, Y. Segawa and K. Itami, *Angew. Chem. Int. Ed.*, 2015, **54**, 3707–3711.
14 J. Xia, J. W. Bacon and R. Jasti, *Chem. Sci.*, 2012, **3**, 3018–3021.
15 T. Iwamoto, Y. Watanabe, T. Sadahiro, T. Haino and S. Yamago, *Angew. Chem. Int. Ed.*, 2011, **50**, 8342–8344.
16 M. Ball and C. Nuckolls, *ACS Cent. Sci.*, 2015, **1**, 416–417.
17 M. Ball, Y. Zhong, B. Fowler, B. Zhang, P. Li, G. Etkin, D. W. Paley, J. Decatur, A. K. Dalsania, H. Li, S. Xiao, F. Ng, M. L. Steigerwald and C. Nuckolls, *J. Am. Chem. Soc.*, 2016, **138**, 12861–12867.
18 P. Neuhaus, A. Cnossen, J. Q. Gong, L. M. Herz and H. L. Anderson, *Angew. Chem. Int. Ed.*, 2015, **54**, 7344–7348.
19 Y. Segawa, A. Fukazawa, S. Matsuura, H. Omachi, S. Yamaguchi, S. Irle and K. Itami, *Org. Biomol. Chem.*, 2012, **10**, 5979–5984.
20 T. Iwamoto, Y. Watanabe, Y. Sakamoto, T. Suzuki and S. Yamago, *J. Am. Chem. Soc.*, 2011, **133**, 8354–8361.
21 V. C. Parekh and P. C. Guha, *J. Indian Chem. Soc.*, 2012, **11**, 95–100.
22 A. Y. Yasutomo Segawa and K. Itami, in *Chemistry of carbon nanostructures*, ed. K. MÃijllen and X. Feng, Walter de Gruyt GmbHer, Berlin/Boston, 2017, ch. Chemical Synthesis of cycloparaphenylenes, pp. 1–148.
23 H. Takaba, H. Omachi, Y. Yamamoto, J. Bouffard and K. Itami, *Angew. Chem. Int. Ed.*, 2009, **48**, 6112–6116.
24 S. Yamago, Y. Watanabe and T. Iwamoto, *Angew. Chem. Int. Ed.*, 2010, **49**, 757–759.
25 K. Eiichi, I. Takahiro, S. Toshiyasu and Y. Shigeru, *Chem. Lett.*, 2013, **42**, 621–623.
26 C. Huang, Y. Huang, N. G. Akhmedov, B. V. Popp, J. L. Petersen and K. K. Wang, *Org. Lett.*, 2014, **16**, 2672–2675.
27 H. Omachi, Y. Segawa and K. Itami, *Org. Lett.*, 2011, **13**, 2480–2483.
28 Y. Ishii, Y. Nakanishi, H. Omachi, S. Matsuura, K. Matsui, H. Shinohara, Y. Segawa and K. Itami, *Chem. Sci.*, 2012, **3**, 2340–2345.
29 T. Kawase and H. Kurata, *Chem. Rev.*, 2006, **106**, 5250–5273.
30 T. Kawase, K. Tanaka, N. Shiono, Y. Seirai and M. Oda, *Angew. Chem. Int. Ed.*, 2004, **43**, 1722–1724.
31 T. Kawase, K. Tanaka, Y. Seirai, N. Shiono and M. Oda, *Angew. Chem. Int. Ed.*, 2003, **42**, 5597–5600.
32 T. Kawase, N. Fujiwara, M. Tsutumi, M. Oda, Y. Maeda, T. Wakahara and T. Akasaka, *Angew. Chem. Int. Ed.*, 2004, **43**, 5060–5062.
33 T. Iwamoto, Y. Watanabe, T. Sadahiro, T. Haino and S. Yamago, *Angew. Chem. Int. Ed.*, 2011, **50**, 8342–8344.
34 P. Della Sala, C. Talotta, T. Caruso, M. De Rosa, A. Soriente, P. Neri and C. Gaeta, *J. Org. Chem.*, 2017, **82**, 9885–9889.
35 S. Solomon, G.-K. Plattner, R. Knutti and P. Friedlingstein, *Proc. Natl. Acad. Sci.*, 2009, **106**, 1704–1709.
36 R. Monastersky, *Nature*, 2013, **497**, 13–14.
37 H. Khatib, *Energy Pol.*, 2012, **48**, 737 – 743.
38 H. Wang and D. Cao, *J. Phys. Chem. C*, 2015, **119**, 6324–6330.
39 S. R. Venna and M. A. Carreon, *J. Am. Chem. Soc.*, 2010, **132**, 76–78.
40 J. Tollefson, *Nature*, 2011, **473**, 134–135.
41 P. Tontiwachwuthikul, A. Meisen and C. Lim, *Chem. Eng. Sci.*, 1992, **47**, 381 – 390.
42 U. E. Aronu, H. F. Svendsen, K. A. Hoff and O. Juliussen, *Energy Procedia*, 2009, **1**, 1051 – 1057.
43 P. Luis, *Desalination*, 2016, **380**, 93 – 99.
44 M. Saleh, H. M. Lee, K. C. Kemp and K. S. Kim, *ACS Appl. Mater. Interfaces*, 2014, **6**, 7325–7333.
45 S. Biswas, D. E. P. Vanpoucke, T. Verstraelen, M. Vandichel, S. Couck, K. Leus, Y.-Y. Liu, M. Waroquier, V. Van Speybroeck, J. F. M. Denayer and P. Van Der Voort, *J. Phys. Chem. C*, 2013, **117**, 22784–22796.
46 M. J. Frisch, G. W. Trucks, H. B. Schlegel, G. E. Scuseria, M. A. Robb, J. R. Cheeseman, G. Scalmani, V. Barone, B. Mennucci, G. A. Petersson, H. Nakatsuji, M. Caricato, X. Li, H. P. Hratchian, A. F. Izmaylov, J. Bloino, G. Zheng, J. L. Sonnenberg, M. Hada, M. Ehara, K. Toyota, R. Fukuda, J. Hasegawa, M. Ishida, T. Nakajima, Y. Honda, O. Kitao, H. Nakai, T. Vreven, J. A. Montgomery, Jr., J. E. Peralta, F. Ogliaro, M. Bearpark, J. J. Heyd, E. Brothers, K. N. Kudin, V. N. Staroverov, R. Kobayashi, J. Normand, K. Raghavachari, A. Rendell, J. C. Burant, S. S. Iyengar, J. Tomasi, M. Cossi, N. Rega, J. M. Millam, M. Klene, J. E. Knox, J. B. Cross, V. Bakken, C. Adamo, J. Jaramillo, R. Gomperts, R. E. Stratmann, O. Yazyev, A. J. Austin, R. Cammi, C. Pomelli, J. W. Ochterski, R. L. Martin, K. Morokuma, V. G. Zakrzewski, G. A. Voth, P. Salvador, J. J. Dannenberg, S. Dapprich, A. D. Daniels, Ö. Farkas, J. B. Foresman, J. V. Ortiz, J. Cioslowski and D. J. Fox, *Gaussian 09 Revision D.01*, Gaussian Inc. Wallingford CT 2009.
47 Y. Zhao and D. G. Truhlar, *Theor. Chem. Acc.*, 2008, **120**, 215–241.
48 F. Weigend and R. Ahlrichs, *Phys. Chem. Chem. Phys.*, 2005, **7**, 3297–3305.
49 F. Weigend, *Phys. Chem. Chem. Phys.*, 2006, **8**, 1057–1065.
50 R. Seeger and J. A. Pople, *J. Chem. Phys.*, 1977, **66**, 3045–3050.
51 R. Bauernschmitt and R. Ahlrichs, *J. Chem. Phys.*, 1996, **104**, 9047–9052.
52 S. Boys and F. Bernardi, *Mol. Phys.*, 1970, **19**, 553–566.
53 R. Bader, *Chem. Revs.*, 1991, **91**, 893.
54 R. F. W. Bader, *Chem. Rev.*, 1991, **91**, 893–928.
55 J. Hernández-Trujillo and R. F. W. Bader, *J. Phys. Chem. A*, 2000, **104**, 1779–1794.
56 R. F. W. Bader, *Acc. Chem. Res.*, 1985, **18**, 9–15.
57 T. Lu and F. Chen, *J. Comput. Chem.*, 2012, **33**, 580–592.
58 J. Xia and R. C. . Jasti, *CCDC 852989. The Cambridge Crystallographic Data Centre*, 2014.
59 P. M. O. Rodrigues, *J. Math. Pures Appl.*, 1840, **5**, 380–440.
60 D. Jose and A. Datta, *J. Phys. Chem. Lett*, 2010, **1**, 1363–1366.
61 T.-A. V. Khuong, G. Zepeda, R. Ruiz, S. I. Khan and M. A. Garcia-Garibay, *Cryst. Growth Des.*, 2004, **4**, 15–18.
62 Z. Dominguez, H. Dang, M. J. Strouse and M. A. Garcia-Garibay, *J. Am. Chem. Soc.*, 2002, **124**, 7719–7727.
63 S. M. Bachrach and D. Stück, *J. Org. Chem.*, 2010, **75**, 6595–6604.
64 Y. Segawa, H. Omachi and K. Itami, *Organic Letters*, 2010, **12**, 2262–2265.
65 K. Matsui, Y. Segawa and K. Itami, *Org. Lett.*, 2012, **14**, 1888–1891.
66 J. M. Van Raden, E. R. Darzi, L. N. Zakharov and R. Jasti, *Org. Biomol. Chem.*, 2016, **14**, 5721–5727.
67 S. Emamian and S. Tayyari, *J. Chem. Sci.*, 2013, **125**, 939–948.
68 T. A. L. O. G. R. B.A. Shainyan, N.N. Chipanina and L. Rosentsveig, *Tetrahedron*, 2010, **66**, 8551–8556.
69 E. M. E. Espinosa and C. Lecomte, *J. Phys. Lett*, 1998, **285**, 170–173.
70 E. R. Johnson, S. Keinan, P. Mori-Sánchez, J. Contreras-García, A. J. Cohen and W. Yang, *J. Am. Chem. Soc.*, 2010, **132**, 6498–6506.
71 R. F. W. Bader and H. Essén, *J. Chem. Phys.*, 1984, **80**, 1943–1960.
72 G. V. Gibbs, D. F. Cox and K. M. Rosso, *J. Phys. Chem. A*, 2004, **108**, 7643–7645.
73 A. Vidal-Vidal, C. Silva López and O. N. Faza, *J. Phys. Chem. A*, 2017, **121**, 9518–9530.
74 A. Vidal-Vidal, O. N. Faza and C. Silva López, *J. Phys. Chem. A*, 2017, **121**, 9118–9130.
75 E. Fermi, *Z. Phys.*, 1931, **71**, 250–259.
76 G. Amat and M. Pimbert, *J. Mol. Spectrosc.*, 1965, **16**, 278 – 290.
77 A. Vidal-Vidal, M. Perez-Rodriguez, J.-P. Torre and M. M. Pineiro, *Phys. Chem. Chem. Phys.*, 2015, **17**, 6963–6975.
78 C. W. McCluskey and D. S. Stoker, *arxiv:physics*, 2006, 0601182.

View Article Online
DOI: 10.1039/C7CP08498F

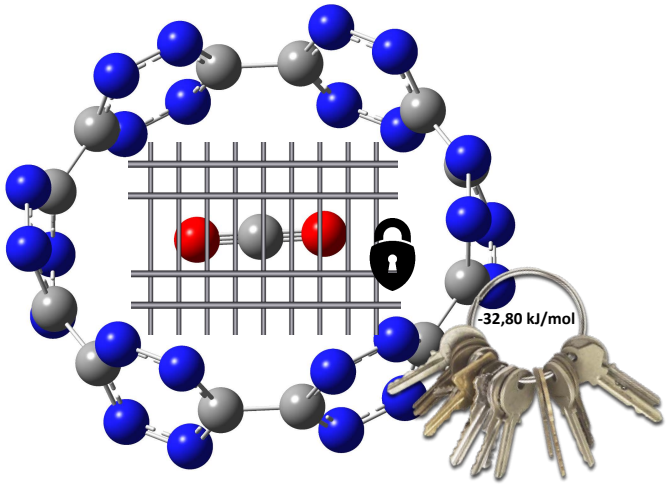

High binding energies, which increase with the number of nitrogens, make nitrogen-doped nanohoops promising CO_2 capturing and sensing devices.